British Journal of Pharmacology 171: 2321-2334 (2014)
DOI: 10.1111/bph.12572

Reversal of SIN-1-induced eNOS dysfunction by the spin trap, DMPO, in bovine aortic endothelial cells *via* eNOS phosphorylation

Amlan Das,[§,a] Bhavani Gopalakrishnan,[§,a] Lawrence J Druhan,[b] Tse-Yao Wang,[a] Francesco De Pascali,[a] Antal Rockenbauer,[e] Ira Racoma,[a] Saradhadevi Varadharaj,[a] Jay L Zweier,[a,c] Arturo J Cardounel[b] and Frederick A Villamena[a,d,*]

[a]*Davis Heart and Lung Research Institute, College of Medicine,* [b]*Department of Anesthesiology,* [c]*Department of Internal Medicine,* [d]*Department of Pharmacology, College of Medicine, The Ohio State University, Columbus, Ohio, 43210,USA*

[e]*Institute of Molecular Pharmacology, Research Centre for Natural Sciences, Hungarian Academy of Sciences, P.O. Box 17, H-15259 Budapest, Hungary*

[§] Both authors equally contributed to this work.

*To whom correspondence should be addressed: Frederick A. Villamena, Davis Heart and Lung Research Institute, Department of Pharmacology, College of Medicine, The Ohio State University, 473 W. 12th Ave., Columbus, Ohio 43210, USA, Tel. No.: (614) 292-8215; E-mail: villamena.1@osu.edu

Summary

Background and Purpose

Nitric oxide (NO) derived from eNOS is mostly responsible for the maintenance of vascular homeostasis where decrease in its bioavailability is characteristic of ROS-induced endothelial dysfunction (ED). Since 5,5-Dimethyl-1-pyrroline-*N*-oxide (DMPO), a commonly used spin trap, has been shown to control intracellular nitroso-redox balance by scavenging ROS and donating NO it was employed as cardio-protective agent against ED but the mechanism of its protection is still not clear. This study elucidates the mechanism of protection imparted by DMPO against SIN-1-induced oxidative injury to bovine aortic endothelial cells (BAEC).

Experimental Approach

BAEC were treated with SIN-1 as $ONOO^-$ donor and post-incubated with DMPO. MTT assay was employed to assess cytotoxicity by SIN-1 and cytoprotection by DMPO. Levels of ROS and NO generation from HEK293 cells transfected with wild type and mutant eNOS cDNAs, BH_4 bioavailability, eNOS activity, eNOS and Akt kinase phosphorylation were determined.

Key Results

Post-treatment of cells with DMPO attenuated SIN-1-mediated cytotoxicity and ROS generation, restoration of NO levels via increased in eNOS activity and phospho-eNOS levels. Treatment with DMPO alone significantly increased NO levels and induced phosphorylation of eNOS S1179 *via* Akt kinase. Transfection studies with wild type and mutant human eNOS confirmed a dual role of eNOS as $O_2^{\bullet-}$ with SIN-1 treatment and NO producer in the presence of DMPO.

Conclusion and Implications

This study demonstrates that post-treatment with DMPO of oxidatively challenged cells can impart reversal of eNOS dysfunction and can have pharmacological implications in the treatment of cardiovascular diseases.

Keywords

eNOS; DMPO; spin trapping; endothelial dysfunction; peroxynitrite; oxidative stress; reactive oxygen species; nitric oxide; cardiovascular diseases; endothelial cells

Introduction

Oxidative stress resulting from the overproduction of reactive oxygen species (ROS), leads to endothelial dysfunction which is implicated in pathophysiology of several cardiovascular disorders (CVD) such as atherosclerosis, hypercholesterolemia, hypertension, Type 2 diabetes, and heart failure (Cai *et al.*, 2000; Heitzer *et al.*, 2001; Vita, 2011). Excessive ROS generation within the vasculature may lead to the oxidation of low-density lipoproteins, decreased bio-availability of endothelium-derived nitric oxide (NO) (O'Donnell *et al.*, 2001) and formation of peroxynitrite ($ONOO^-$), a highly reactive molecule (Beckman *et al.*, 1996). All these events are attributed to the impairment of the vascular endothelium function.

Endothelium –derived nitric oxide (NO) is an important signaling molecule which regulates the vessel homeostasis by inducing vascular smooth muscle relaxation, and inhibiting vascular smooth muscle hypertrophy, regulating platelet aggregation, and leukocyte adhesion (Gross *et al.*, 1995). In the endothelium, NO is produced by a family of enzymes termed nitric oxide synthases (NOSs) that catalyze the conversion of L-arginine to L-citrulline and NO. The reactive oxygen and nitrogen species generated during oxidative stress are known to induce eNOS dysfunction that leads to the uncoupling of the enzyme and results in the production of NOS-derived $O_2^{\bullet-}$ instead of NO (Wei *et al.*, 2003). The resulting imbalance between NO and $O_2^{\bullet-}$ can contribute to the onset of a variety of cardiovascular diseases.

NOS activity is regulated by a complex cascade of phosphorylation/de-phosphorylation at particular regulatory residues in the enzyme. Phosphorylation of eNOS S635 and S1179 leads to the activation of eNOS function while phosphorylation at

threonine 497 downregulates it (Harris *et al.*, 2001; Michell *et al.*, 2001). Activation by eNOS S1179 phosphorylation results from the enhanced electron flux through the reductase domain and inhibition of calmodulin-dissociation from the enzyme in a calcium-independent fashion (Fulton *et al.*, 1999; McCabe *et al.*, 2000) andis mediated by several upstream kinases, among which PI3/Akt has been reported to play a crucial role in the regulation of enzyme activity (Fulton *et al.*, 1999).

Most of the NO donor drugs are limited only by their NO delivering property and usually exhibit uncontrolled delivery of NO due to their instability in blood plasma (Wang *et al.*, 2005). Nitrones can both scavenge reactive species (Villamena *et al.*, 2005; Villamena *et al.*, 2004) and also exhibit controlled release of NO as a consequence (Locigno *et al.*, 2005; Nash *et al.*, 2012), and is therefore, more desirable and unique among current drugs. To date, there are two major types of nitrones: the cyclic nitrones which include 5,5-dimethyl-1-pyrroline-*N*-oxide (DMPO), 5-carbamoyl-5-methyl-1-pyrroline-*N*-oxide (AMPO), 5-ethoxycarbonyl-5-methyl-1-pyrroline-*N*-oxide (EMPO), 5-(diethoxyphosphoryl)-5-methyl-1-pyrroline-*N*-oxide (DEPMPO), and the linear nitrones (PBN and NXY-059) α-phenyl-*N*-*tert*-butylnitrone (PBN), (disodium-[(*tert*-butylimino) methyl] benzene-1,3-disulfonate *N*-oxide (NXY-059) which have been used to detect free

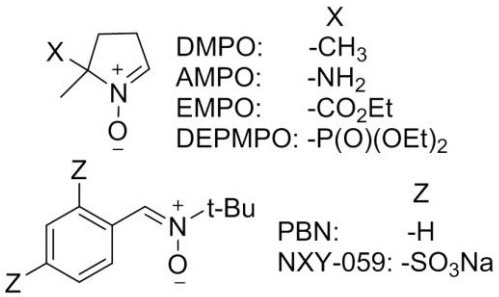

radicals. Nitrones though structurally simple molecules, yet they possess rich chemistries, and biological properties that make them important pharmacological agents (Das *et al.*, 2012; Traynham *et al.*, 2012; Villamena *et al.*, 2012; Zamora *et al.*, 2013; Zuo *et al.*, 2009). Nitrone spin traps such as DMPO, PBN and its derivative, NXY-059 have shown pharmacological activity against ischemia and reperfusion (I/R) injury in the heart and brain (Floyd, 2009; Zuo *et al.*, 2009), neurodegeneration (Floyd *et al.*) and cancer (Floyd, 2009; Floyd *et al.*, 2008). NXY-059 was the first neuroprotective agent that reached a clinical trial phase in the USA (Floyd *et al.*, 2008). Application of DMPO as a cardio-protective agent was previously reported *(*Tosaki et al., *1990)* but its modes of action were unclear. DMPO also confered protection against cardiac IR injury in Langendorff rat heart preparations by salvaging the METC complexes and decreased ROS production (Zuo *et al.*, 2009). Other experimental evidences suggest involvement of other mechanisms for cardioprotection by DMPO other than its direct spin trapping properties such as induction of phase II enzymes *via* Nrf-2 nuclear translocation; and suppression of mitochondria-dependent pro-apoptotic signaling in endothelial cells (Das *et al.*, 2012). Increase in mycoyte contraction *via* regulation of nitroso-redox levels and increase in sarcoplasmic reticulum Ca^{2+} handling have also been proposed (Traynham *et al.*, 2012). Although several works already described the reversal of eNOS uncoupling *via* supplementation with tetrahydrobiopterin (Forstermann, 2006), in the present study, we explored the mechanism of reversal of eNOS dysfunction by post-treatment of endothelial cells with DMPO after treating the cells with the peroxynitrite donor, SIN-1, offering another mechanistic insights into the cardioprotective property of nitrones.

Methods

Cell culture and maintenance

BAEC were cultured using a T75 cm^2 flask in DMEM medium with 1g/L D-glucose and 4 mM L-glutamine, and supplemented with 10% fetal bovine serum, 50 μg/mL pencillin, 50 μg/mL streptomycin, 2.5 mg/L endothelial cell growth supplement, and 1% MEM-non essential amino acids at 37°C in a humidified atmosphere of 5% CO_2 and 20% O_2. HEK293 (human embryonic kidney) were cultured under same conditions in DMEM media without endothelial cell growth supplement, and MEM-non essential amino acids. The medium was changed every 2-3 days and cells were sub-cultured once they reached 90-95% confluence or 80% for HEK293 cells.

SIN-1 and DMPO treatment of cells

BAEC or HEK293 were seeded at a density of 10^4 cells/mL in each well using a 24-well plate and grown to 70% confluency. Cells were treated with 500 μM SIN-1 for 2 h, and then post-incubated in plain medium without SIN-1 for additional 24 h, in the absence or presence of DMPO. For the cytoprotection studies, cells were treated with 500 μM SIN-1 for 2 h and subsequently post-incubated with DMPO for 24 h. Cell viability was assessed by MTT assay following the protocol described previously (Das *et al.*, 2010). Cell viability was calculated as the percentage of inhibition by the following formula (equation 1) :

$$\% \text{ inhibition} = [1-A_t/A_s] \times 100\% \quad (1)$$

where A_t and A_s are absorbance of the sample and solvent alone, respectively. Results were presented as mean ± SEM, where n = 6.

ROS detection by confocal microscopy

Cells with density of 10^4 cells/mL were seeded on sterile glass cover slips 6-well plate. Treated cells were fixed with 10% para-formaldehyde at room temperature for 10 min, washed with PBS three times and subsequently incubated with 25 μM of the fluorogenic probe DCFH-DA or 10 μM DHE for 30 min at 37°C, followed by nuclei staining with DAPI (1 μM) for 30 min. Images were then captured by Olympus FluoView-1000 confocal microscope using an excitation/emission filter of 543/602 nm for DHE, 488/535 nm for DCFH-DA and 405/422 nm for DAPI. Fluorescence intensities of 100 cells from different fields were calculated and results were presented as mean ± SEM of three independent experiments (n = 3).

ROS and NO detection by EPR spin trapping

Cells (10^4 cells/mL) were grown to 70 % confluency in 6-well plates. After SIN-1 treatment, cells were incubated with 150 μl of EMPO (25 mM) and 150 μl of Me-β-CD (50 mM) and 10 μl of 10 μM CaI for 15 min (Šnyrychová, 2010). The supernatant (300 μl) was transferred to a quartz flat cell and spin adduct formation was detected at room temperature using Bruker EMX X-Band EPR spectrometer. Experiment was repeated in the presence or absence of DMPO post-incubation. Instrument parameters were as follows: microwave frequency, 9.8 GHz; center field, 3485 G; modulation amplitude, 0.2-1.0 G; microwave power, 10 mW; conversion time: 41 ms; time constant: 82 ms, sweep time: 42 s; sweep width: 120 G; receiver gain, 1 x 10^5 and using incremental sweep. Spectra were simulated using an automatic fitting program (Rockenbauer *et al.*,

1996) where the pertinent hfsc's of $HO_2^{\bullet}$, $HO^{\bullet}$ and C-centered adducts and their concentrations from the total area of each spectrum were obtained. Adducts were independently prepared using hypoxanthine-xanthine oxidase, Fe^{2+}-H_2O_2 and Fe^{2+}-H_2O_2-ethanol for $HO_2^{\bullet}$, $HO^{\bullet}$ and C-centered adducts respectively (Table S3). Spectra were obtained from three independent experiments (n = 3). Using the same cell cultures in 6-well plates, generation of NO in cells were detected by EPR spin trapping using $Fe(MGD)_2$ as the spin trap following the published protocol (Gopalakrishnan *et al.*, 2012). Cells were washed with PBS after treatment, then incubated for 15 minutes with PBS with $CaCl_2$ and $MgCl_2$, calcium ionophore A21387 (10 μM), $FeSO_4$ (3.5 mM), and ammonium N-methyl-D-glucamine dithiocarbamate complex NH_4MGD (20.8 mM) at a final volume of 500 μL. The supernatant (300 μl) was transferred to a quartz flat cell and spin adduct formation was detected at room temperature with EPR instrument parameters: microwave frequency, 9.8 GHz; center field, 3426.5 G; modulation amplitude, 6 G; microwave power, 12 mW; conversion time: 10 ms; time constant: 20 ms, sweep time: 10 s; sweep width: 100 G; receiver gain, 1 x 10^5 and using incremental sweep. The 2-D spectra were integrated and baseline corrected using Bruker WinEPR data processing software. Results are as mean ± SEM of three independent experiments (n = 3).

BAEC in a T75 cm^2 culture flask were serum-starved overnight then endogenous L-[^{14}N]-arginine was exchanged for L-[^{15}N]-arginine by incubating cells with Tyrode's solution supplemented with 84 mg/L L-[^{15}N]-arginine for 30 min at 37° C. After incubation, cells were washed with PBS, treated with $Fe(MGD)_2$ as above and EPR spectra were acquired (Gopalakrishnan *et al.*, 2012).

Determination of eNOS activity

eNOS activity was determined using the conversion of arginine to citrulline assay with [^{14}C]arginine as a substrate using the previously published protocol with a slight modification (Giraldez *et al.*, 1998). Cultured BAEC (10^4 cells/ mL) were grown to 70 % confluency in T75 cm^2 culture flask and subjected to SIN-1 treatment and DMPO post-treatment. After treatment, eNOS activity was measured by L-[^{14}C]arginine to L-[^{14}C]citrulline conversion in a total volume of 50 µL buffer containing 50 mM Tris-HCl, pH 7.4, 1 µM L-[^{14}C]arginine, 1 mM NADPH, 0.6 mM Ca^{2+}, 2.5µM calmodulin, and 10 µM BH_4. After 10 min incubation at 37°C, the mixture was terminated by adding 400 µL of stop buffer (20 mM HEPES, pH 5.5, 2 mM EDTA, 2 mM EGTA). L-[^{14}C]citrulline was separated by mixing the reaction mixtures with 100 µL of pre-equilibrated Dowex AG 50W-X8 (Na^+ form) cation exchange resin, then passed through spin columns and quantitated by liquid scintillation counter. Results were presented as mean ± SEM of three independent experiments (n = 3).

Measurement of BH_4 by HPLC chromatography

The total BH_4 was measured using HPLC analysis as described elsewhere (Dumitrescu *et al.*, 2007; Hyland, 1985). Cells were grown in T75 cm^2 flask up to 70% confluency. SIN-1 treated cells were washed once with PBS and lysed with lysis buffer containing 1 mM ascorbate, 1 mM DTT and 100 µM DTPA, followed by sonication. The mixture was then centrifuged at 12000 x g for 1 min at 4 ^oC. The supernatant containing the protein was removed by filtration through a Microcom YM-3 spin column. The

filtrates were injected to an ESA HPLC system with a C-18 column (T3 4.6 x 150 mm 5 micron) and HPLC separation was performed following the published protocol (Dumitrescu *et al.*, 2007; Hyland, 1985) using mobile phase comprising of 50 mM potassium phosphate, 10 mM phosphate monobase, 12% ACN, 6 mM citric acid, 1 mM DTT, 5 mM octyl sulfate, pH 3 and isocratic elution at 1.2 mL/min. Detection parameters are: 35mV and 500mV for electrochemical cell; fluorescence: excitation at 348 nm and emission at 444 nm; UV at 254 nm. Results were presented as mean ± SEM of three independent experiments (n = 3).

Western blot analysis

Western blot analysis was performed to determine the expression levels of p-eNOS, p-Akt, t-Akt and t-eNOS proteins in untreated, SIN-1 treated, and nitrone-post incubated SIN-1 treated BAEC. Prior to treatment, cultured BAEC (10^4 cells/ mL) were grown to 70 % confluency on 60 mm petri-dishes, and 50 µg of protein from each set was used for western blotting. In a separate experimental set, the membrane was incubated with mouse monoclonal anti-p-eNOS (S1179) antibody (1:1000 dilution), mouse monoclonal anti p-Akt (Ser-473) antibody (1:500 dilution), mouse monoclonal anti-t-eNOS antibody (1:1000 dilution), mouse monoclonal anti-t-Akt antibody (1:500 dilution) and mouse monoclonal anti-β-actin antibody (1:1000 dilution) overnight at 4 ^{o}C. The protein bands were visualized using chemiluminiscence kit available commercially and the bands were quantified densitometrically using available software.

Transient transfection of HEK293 cells with wild type and mutant eNOS cDNAs

Human embryonic kidney cells were transfected with 5 μg/μl of eNOS cDNA (wild type and mutant where S1179 was changed to alanine) (Lin *et al.*, 2003) using Lipofectamine ^{TM} 2000 (Invitrogen) as per manufacturer's instruction. The transfection efficiency was analyzed using western blot analysis of eNOS proteins and by measuring NO levels.

Statistical analysis

Data are presented as the mean of at least three independent experiments along with standard error of the mean (SEM). Statistical analysis of data was done by one-way analysis of variance (ANOVA), with Student-Newman-Keul test by using Sigma plot 12.0. The *p* value <0.05 was considered to be statistically significant.

Results

Dose- and time-dependent cytoprotective effects from post-treatment by DMPO of SIN-1-challenged BAEC

Treatment of cells with varying concentrations of DMPO alone (25- 500 μM) for 24 h did not result in loss of cell viability (Figure S1). However, cells challenged with 500 μM SIN-1 at varying time periods resulted in significant cytotoxicity (Figure S2). A 50% decrease in cell viability was observed after 2 h of SIN-1 treatment followed by 24 h of post-incubation in plain media (without SIN-1) (Figure S2). SIN-1 has been suggested to induce cell death *via* two mechanisms, production of peroxynitrite ($ONOO^-$) through reaction between NO and $O_2^{\bullet -}$ to finally form $HO^\bullet$ (Ishii *et al.*, 1999), and generation of H_2O_2 (Lomonosova *et al.*, 1998). When SIN-1-challenged cells were

post-incubated with DMPO, significant increase in cell viability was observed in both dose- and time-dependent fashion (Figures 1A and 1B). Highest cytoprotection was observed when SIN-1 treated cells were post-incubated with 100 μM of DMPO for 24 h compared to pre-treatment of BAEC with DMPO for 24 hours prior to 2 h SIN-1 treatment that shows no significant reduction in cell viability (data not shown). Hence, from here onwards, cells will be post-treated with 100 μM of DMPO after SIN-1 challenge.

Attenuation of ROS generation in SIN-1-treated BAEC by DMPO

To test if cells generate $O_2^{\bullet-}$ after treatment with SIN-1, EPR spin trapping was performed using EMPO/Me-β–CD as spin trap on SIN-1-treated BAEC at various times (0-24 h) of incubation. EPR results showed increased ROS intensities with increasing time of post-incubation along with the formation of a C-centered adduct which could be formed as secondary products (Figure S3A and Table S1 for the simulation). The low-field peak intensity of the EPR spectra increased significantly in SIN-1 treated cells by up to 2.9-fold after 24 h of post-incubation (Figure S3B). EPR results were confirmed by confocal microscopy using DHE staining of SIN-1-treated cells at different time points. Treatment of cells with SIN-1 for 2 h (corresponding to 0 h of post-incubation) resulted in a significant increase of DHE-fluorescence specific for $O_2^{\bullet-}$ and the signal remained persistent for up to 6 h of post-incubation in plain media with fluorescence decreases upon further incubation for 12 h and 24 h (Figure S4).

Since H_2O_2 could be also form from SIN-1 treatment *via* $O_2^{\bullet-}$ dismutation (Lomonosova *et al.*, 1998), we performed a time-dependent confocal microscopy study

on SIN-1-treated BAEC by staining the cells with H_2O_2-specific fluorescent probe, CM-DCFDAHE (Figure S5). SIN-1-untreated BAEC showed no detectable DCF-fluorescence signal indicating that the cells did not produce H_2O_2. However, when BAEC were treated with SIN-1 for 2 h and post-incubated for an additional 24 h, a time-dependent accumulation of DCF-fluorescence signal was detected (Figure S5).

When SIN-1-challenged cells were post-treated with 100 μM DMPO, DCF-fluorescence intensity was found to be significantly decreased (Figures 2A and 2B) compared to a 3-fold increase in DCF- fluorescence in SIN-1 treated cells without DMPO post-treatment. Simulation of the EPR spectra also revealed that the concentration of O-centered adduct was significantly decreased with a concomitant decrease in the concentration of C-centered adducts when SIN-1-treated BAEC were post-incubated with DMPO for 24 h (Table S2 and Figures 2C-2D.

Restoration of NO bioavailability in SIN-1-treated BAEC by DMPO

Since oxidative stress leads to decreased bioavailability of NO (Cai *et al.*, 2000), the effect of SIN-1 on NO production in BAEC was investigated. Using EPR and $Fe(MGD)_2$ as spin trap to detect NO generation (Figures 3A and 3B), a significant decrease in NO production of almost 50% was observed when cells were treated with SIN-1 for 2 h and post-incubated in plain media for 24 h. The same observation was previously reported for BAEC upon treatment with SIN-1 or $ONOO^-$ (Kuzkaya *et al.*, 2003). However, post-treatment with DMPO for 24 h resulted in the restoration of the NO levels by about 35%. Treatment of cells with the NOS inhibitor L-NAME,

completely abolished the NO-signal (Figure 3B) indicating an eNOS-derived NO production.

Restoration of eNOS activity in SIN-1-treated BAEC by DMPO

eNOS activity was assessed using the L-[^{14}C] arginine to L-[^{14}C] citrulline conversion assay. BAEC were treated with SIN-1 for 2 h and post-incubated for another 24 h that resulted in significant inhibition of eNOS activity by ~30%. However, post-treatment with DMPO for 24 h led to the complete restoration of eNOS activity (Figure 3C). This provides definitive evidence that the effects of DMPO on NO production are mediated at least in part through increased eNOS-derived NO production and not merely a consequence of scavenging SIN-1-derived superoxide.

Increased bioavailability of NO in BAEC treated with DMPO alone

Since post-treatment with DMPO resulted in a significant increase in NO production and NOS activity in SIN-challenged cells, we investigated if the nitrone alone could increase NO generation in BAEC without oxidatively challenging the cells. EPR studies revealed that treatment of cells with DMPO resulted in a time-dependent increase in cellular NO and a 40% increase in NO production was observed after 24 h of treatment (Figure 4).

Determination of NO source: nitrone versus L-Arginine

To determine if the source of the generated NO is through nitrone-decomposition (Locigno *et al.*, 2005) or eNOS-catalyzed conversion of L-arginine to L-citrulline, an

isotope-labeling experiment using L-[^{15}N]-arginine was carried out. Due to the difference in the nuclear spins of ^{14}N (I = ″) and ^{15}N (I = 1), it is therefore possible to monitor the source of NO (Xia *et al.*, 1997). A time-dependent formation of a doublet signal, characteristic of ^{15}NO–Fe–MGD spectrum was observed (Figure 5A) after incubation of L-[^{14}N]-arginine-depleted BAEC with L-[^{15}N]-arginine for 24 h. Incubation of cells in the presence of DMPO and L-[^{15}N]-arginine for 24 h gave a similar doublet spectrum demonstrating that most of the detected NO were generated from the ^{15}N-labeled arginine (Figure 5B). This result suggests that the NO generated in BAEC upon DMPO-treatment did not originate from the nitrone itself, but rather from the metabolism of L-arginine to L-citrulline, and thus, implicates NOS as the source of the NO.

Induction of eNOS- and Akt-phosphorylation in BAEC by DMPO in the absence of SIN-1 treatment

Western blot was performed to detect p-eNOS S1179 in BAEC treated with DMPO for 12 h and 24 h. A time-dependent increase in p-eNOS levels was observed due to DMPO treatment with a significant 2.2-fold increase after 12 h of incubation. The p-eNOS level was found to be slightly increased after 24 h of treatment (Figures 6A and 6B). Since protein kinase B or Akt is known to be an upstream regulator of eNOS and results in the phosphorylation of the enzyme (Fulton *et al.*, 1999), p-Akt (Ser-473) levels were also measured in the presence of DMPO. DMPO treatment of cells resulted in a similar time-dependent increase in p-Akt levels. Incubation of cells with DMPO for 12 h and 24 h resulted in 2.7- and 3.5 fold increases in p-Akt levels, respectively (Figures 6A

and 6C). Therefore, these observations show that DMPO can increase NO-bioavailability in BAEC *via* phosphorylation of Akt and eNOS.

Inhibition of SIN-1-mediated down-regulation of p-eNOS and p-Akt in BAEC by DMPO

The phosphorylation levels of eNOS increased by 22% after 2 h of SIN-1 treatment (corresponding to 0 h of post-incubation with DMPO) but there was a time-dependent decrease in p-eNOS levels during further incubation of SIN-1 treated cells in plain media. After 24 h of post-incubation, the p-eNOS band intensity decreased by 55 % compared to control cells (Figures 7A and 7B). However, when SIN-1-challenged cells were post-treated with DMPO for 24 h, p-eNOS levels were significantly restored (Figures 7C and 7D). In addition, we also observed significant restoration of p-Akt levels in SIN-1-treated BAEC upon post-treatment with DMPO (Figures 7C and 7E). These observations show that DMPO can increase NO-bioavailability in SIN-1-challenged BAEC *via* phosphorylation of Akt and eNOS.

SIN-1 mediated eNOS dysfunction is independent of BH_4 depletion

Treatment of BAEC with SIN-1 for 2 h in the absence of DMPO resulted in the depletion of BH_4-levels but upon incubation in plain media for additional 24 h, BH_4-levels were restored in SIN-1 challenged cells (Figure S6). This indicates that BH_4 is metabolically replenished after 24 h of incubation, and therefore, is independent of DMPO action. We also investigated the effect of DMPO on BH_4 state within an hour of

SIN-1 administration to the cell but showed no significant change in the BH_4 levels similar to in the absence of DMPO.

Dual roles of eNOS as target for both SIN-1 and DMPO

HEK293 cells were transfected with the cDNAs encoding both wild type and mutant (S1179A) bovine eNOS. This mutant eNOS was reported to be resistant to phosphorylation and also did not exhibit any Akt-dependent increase in NO-generation (Fulton *et al.*, 1999). Western blot results show equal transfection efficiency for both wild type and mutant eNOS (Figure S7B) but no NO generation from mutant eNOS and with NO generation in wild-type eNOS-transfected cells were observed (Figure S7A). When HEK293 cells were transfected with wild type and mutant eNOS plasmids and were treated with SIN-1 for 2 h, formation of $O_2^{\bullet-}$ was observed using DHE-staining of the cells transfected with wild type eNOS-plasmid, whereas in mutant eNOS transfected cells, $O_2^{\bullet-}$ generation is much lower (Figure 8A-8C). EPR spin trapping to detect ROS generation in mutant eNOS-transfected cells gave low levels of ROS even with SIN-1 or DMPO treatment (Figure 8D) confirming the role of eNOS S1179 in radical generation. It has been shown that phosphorylation of eNOS S1177 at low Ca^{2+} concentrations is critical for $O_2^{\bullet-}$ generation (Chen *et al.*, 2008).

To investigate whether DMPO can attenuate SIN-1 mediated ROS generation in HEK293 cells transfected with wild type or mutant eNOS-plasmid, confocal microscopy using DCF-DA stain was employed to detect ROS generation and revealed that SIN-treatment gave a ~4.4-fold increase in DCF-fluorescence intensity and is significantly reduced on post-treatment with DMPO (Figure S8A-8B).

Discussion

Oxidative insult to eNOS can reverse its function from being an NO generator to a pro-oxidative enzyme, thereby exacerbating the degenerative processes that have been associated with endothelial dysfunction (Cai *et al.*, 2000). In this work, we demonstrated how DMPO can reverse eNOS function from being pro-oxidative to that of its normal NO synthase function by exploiting the nitrone's ability to regulate the nitroso-redox balance in the cell by scavenging ROS, increasing NO bioavailability, and ultimately eNOS phosphorylation.

Post-treatment by DMPO of SIN-1-challenged BAEC conferred cytoprotection and restored NO production, while post-incubation of BAEC with SIN-1 for an additional 24 h in plain medium (in the absence of DMPO) gradually increased the oxidative burden on the cells. Production of $ONOO^-$ *via* formation of ROS and NO had been implicated in SIN-1 cytotoxicity to endothelial cells (Ishii *et al.*, 1999). Although nitrones are known to react with $ONOO^-$, where $ONOO^-$/ONOOH mediates the formation of the spin adducts using DMPO as spin trap (Gatti *et al.*, 1998; Nash *et al.*, 2012), the possibility that DMPO may be converting SIN-1 as an NO donor rather than a $ONOO^-$ *via* $O_2^{\bullet-}$ scavenging is unlikely since two hours of SIN-1 incubation with cells would not allow $ONOO^-$ to persist due to its short half-life (1.9 sec at pH 7.4) (Beckman *et al.*, 1990) especially in the presence of biological milieu. Furthermore, fluorescence studies showed that the half-time for the steady state $ONOO^-$ production from SIN-1 range from 14 min to 26 min (Martin-Romero *et al.*, 2004). One could envision that after 2 hour incubation of cells with SIN-1, $ONOO^-$ is released into the cell and could have had reacted already causing oxidative damage perhaps to eNOS. Therefore, the observed ROS adducts

formation during spin trapping is not a direct reaction of $ONOO^-$ with DMPO. These results clearly suggest that post-treatment of cells with DMPO attenuates ROS production in SIN-1-treated endothelial cells *via* eNOS dysfunction.

ROS-derived $ONOO^-$ limits bioavailability of the eNOS cofactor, BH_4, resulting from either BH_4-depletion or oxidation thereby resulting to eNOS dysfunction (Kuzkaya *et al.,* 2003)**.** Previous studies also showed that in BAEC, co-incubation of BH_4 or ascorbic acid with SIN-1 can reverse the effect of SIN-1 on NO production perhaps *via* replenishment of oxidized BH_4 or reversal in the oxidation state of the redox-modified BH_4 (Kuzkaya *et al.,* 2003; Vasquez-Vivar *et al.,* 2002; Xia *et al.,* 1998). However, unlike ascorbic acid (Kuzkaya *et al.,* 2003), DMPO does not reverse eNOS function through restoration of BH_4 levels during initial and 24 hours of SIN-1 treatments, and that the observed reduced NO and increase ROS productions could be a result of other mechanisms other than uncoupling due to BH_4 oxidation.

Therefore, the role of eNOS activation *via* phosphorylation was investigated to explain the observed increase in NO production in DMPO-treated cells. Phosphorylation of eNOS S1179 is known to activate eNOS by stimulating the flux of electrons within the reductase domain (Harris *et al.,* 2001; McCabe *et al.,* 2000; Michell *et al.,* 2001). Under oxidative stress conditions, eNOS generates $O_2^{\bullet-}$ and phosphorylation of eNOS S1179 is inhibited leading to decrease in NO production. How phosphorylation of eNOS S1179 is regulated to maintain the $O_2^{\bullet-}$-NO balance under oxidative stress conditions is not completely understood (Xia *et al.,* 1996) but it has been proposed that eNOS phosphorylation is redox-sensitive and is activated by PI3K/Akt pathway (Dimmeler *et al.,* 1999; Fulton *et al.,* 1999) and by other kinases (Alhosin *et al.,* 2013). Regulation of

ATP levels and activation of other kinases such as p38 MAPK and JNK by DMPO, therefore, warrants further investigation. This study, nevertheless, demonstrates that DMPO can reverse eNOS dysfunction through decreased ROS production, increased in NO bioavailability and increased phosphorylation of eNOS S1179 Akt activation.

Traditional antioxidants such as ascobic acid and *N*-acetyl cysteine have been explored for their ability to prevent or reverse eNOS uncoupling in BAEC (Kuzkaya *et al.*, 2003) and in diabetic rat hearts (Okazaki *et al.*, 2011) through an increase in the BH_4/BH_2 ratio. Recently, lipophilic NO-donor and lipophilic antioxidants, when introduced as a hybrid molecule and not as a mixture, can exhibit cardiac protection from I/R through significant reduction of infarct size with improved recovery of cardiac function (Rastaldo *et al.*, 2012), however, the mechanism of this protection was not clear. Moreover, magnesium lithospermate B have been shown to protect endothelium from hyperglycemia-induced dysfunction *via* eNOS phosphorylation, and induction of phase II enzymes by Nrf-2 nuclear translocation, while α-lipoic acid was claimed to be not able to cause these effects (Traynham *et al.*, 2012).

Cardiometabolic disease is a growing health problem that is a combination of various risk factors such as hypertension, hyperglycemia and elevated plasma triglyceride levels, leading to the development of Type 2 diabetes and cardiovascular diseases. While the antioxidants mentioned above could be promising, their therapeutic application could be limited in the treatment of cardiometabolic diseases since unlike nitrones, their modes of action may only be limited to few mechanisms (Zamora *et al.*, 2013). Findings presented in this present work and in our past studies (Das *et al.*, 2012; Durand *et al.*, 2009; Traynham *et al.*, 2012; Zuo *et al.*, 2009) showed that nitrones offer opportunities

for the application of nitrones in the treatment of cardiometabolic disorders such as hypertension and hyperglycemia which are associated with endothelial dysfunction and depletion of cellular antioxidant pool since nitrones do not only scavenge ROS (Durand *et al.*, 2008; Durand *et al.*, 2009) but also acts through NO donation (Locigno *et al.*, 2005); salvaging METC activity (Zuo *et al.*, 2009); increase METC biogenesis (Zuo *et al.*, 2009); inhibition of mitochondrial polarization leading to down regulation of pro-apoptotic signaling pathways; induction of phase II enzyme activities *via* NRF-2 nuclear translocation (Das *et al.*, 2012); increased myocyte contraction *via* increased sarcoplasmic reticulum Ca^{2+} handling (Traynham *et al.*, 2012) and in this study, reversal of eNOS dysfunction.

Future work needs to investigate how DMPO activates Akt by immuno-spin trapping of the relevant proteins and role of nitrones as a potential phosphatase inhibitor, since protein phosphatase 2A (PP2A) was also reported to decrease eNOS S1179 phosphorylation. Therefore, therapeutic agents that can target cytosolic matrix and affect kinase mediated phosphorylation processes in the cell may be able to up-regulate eNOS. Attempts had been made to conjugate cyclic nitrones to several target specific groups in order to facilitate their delivery to specific subcellular compartments (Durand *et al.*, 2010; Durand *et al.*, 2003; Durand *et al.*, 2009) since the poor target specificity of some of the natural antioxidants such as vitamin E, vitamin C, or lipoic acid are limiting their applications against ROS-induced CVDs (Kizhakekuttu *et al.*, 2010; Shay *et al.*, 2009; Willcox *et al.*, 2008). Considering that eNOS is mostly localized near the cell membrane and that mitochondria and sarcoplasmic reticulum are mostly cytosolic, the use of nitrones that can specifically target these compartments can provide opportunities

to identifying which targeted cellular event/s contributes the greatest to I/R injury and which target-specific nitrone will exhibit the most robust protection can give valuable insights into the mechanisms of nitrone protection. To date, targeting oxidative stress at the site/s of their origination still remains an attractive strategy for cardiovascular prevention and therapy (Munzel *et al.*, 2010). Therefore, deeper understanding of radical sources and mechanisms of oxidative stress, and the development of more target specific antioxidants with multi-functional action such as those exhibited by nitrones are necessary.

Acknowledgements

This work was funded by the NIH National Heart, Lung, and Blood Institute grant RO1 HL81248.

References

Alhosin M, Anselm E, Rashid S, Kim JH, Madeira SV, Bronner C, *et al.* (2013). Redox-sensitive up-regulation of eNOS by purple grape juice in endothelial cells: role of PI3-kinase/Akt, p38 MAPK, JNK, FoxO1 and FoxO3a. *PLoS One* **8:** e57883.

Beckman JS, Beckman TW, Chen J, Marshall PA, Freeman BA (1990). Apparent hydroxyl radical production by peroxynitrite: implications for endothelial injury from nitric oxide and superoxide. *Proc Natl Acad Sci U S A* **87:** 1620-1624.

Beckman JS, Koppenol WH (1996). Nitric oxide, superoxide, and peroxynitrite: the good, the bad, and ugly. *Am J Physiol* **271:** 1424-1437.

Cai H, Harrison DG (2000). Endothelial dysfunction in cardiovascular diseases: the role of oxidant stress. *Circ Res* **87:** 840-844.

Chen CA, Druhan LJ, Varadharaj S, Chen YR, Zweier JL (2008). Phosphorylation of endothelial nitric-oxide synthase regulates superoxide generation from the enzyme. *J Biol Chem* **283:** 27038-47.

Das A, Chakrabarty S, Choudhury D, Chakrabarti G (2010). 1,4-Benzoquinone (PBQ) induced toxicity in lung epithelial cells is mediated by the disruption of the microtubule network and activation of caspase-3. *Chem Res Toxicol* **23:** 1054-1066.

Das A, Gopalakrishnan B, Voss OH, Doseff AI, Villamena FA (2012). Inhibition of ROS-induced apoptosis in endothelial cells by nitrone spin traps via induction of phase II enzymes and suppression of mitochondria-dependent pro-apoptotic signaling. *Biochem Pharmacol* **84:** 486-497.

Dimmeler S, Fleming I, Fisslthaler B, Hermann C, Busse R, Zeiher AM (1999). Activation of nitric oxide synthase in endothelial cells by Akt-dependent phosphorylation. *Nature* **399:** 601-5.

Dumitrescu C, Biondi R, Xia Y, Cardounel AJ, Druhan LJ, Ambrosio G, *et al.* (2007). Myocardial ischemia results in tetrahydrobiopterin (BH4) oxidation with impaired endothelial function ameliorated by BH4. *Proc Natl Acad Sci U S A* **104:** 15081-15086.

Durand G, Choteau F, Pucci B, Villamena FA (2008). Reactivity of superoxide radical anion and hydroperoxyl radical with alpha-phenyl-N-tert-butylnitrone (PBN) derivatives. *J Phys Chem A* **112:** 12498-12509.

Durand G, Poeggeler B, Ortial S, Polidori A, Villamena FA, Boker J, *et al.* (2010). Amphiphilic amide nitrones: A new class of protective agents acting as modifiers of mitochondrial metabolism. *J Med Chem* **53:** 4849-4861.

Durand G, Polidori A, Salles JP, Pucci B (2003). Synthesis of a new family of glycolipidic nitrones as potential antioxidant drugs for neurodegenerative disorders. *Bioorg Med Chem Lett* **13:** 859-862.

Durand G, Prosak RA, Han Y, Ortial S, Rockenbauer A, Pucci B, *et al.* (2009). Spin trapping and cytoprotective properties of fluorinated amphiphilic carrier conjugates of cyclic versus linear nitrones. *Chem Res Toxicol* **22:** 1570-1581.

Floyd RA (2009). Serendipitous findings while researching oxygen free radicals. *Free Radic Biol Med* **46:** 1004-1013.

Floyd RA, Castro Faria Neto HC, Zimmerman GA, Hensley K, Towner RA Nitrone-based therapeutics for neurodegenerative diseases: Their use alone or in combination with lanthionines. *Free Radic Biol Med***:** http://dx.doi.org/10.1016/j.freeradbiomed.2013.01.033.

Floyd RA, Kopke RD, Choi CH, Foster SB, Doblas S, Towner RA (2008). Nitrones as therapeutics. *Free Radic Biol Med* **45:** 1361-1374.

Forstermann U (2006). Janus-faced role of endothelial NO synthase in vascular disease: uncoupling of oxygen reduction from NO synthesis and its pharmacological reversal. *Biol Chem* **387:** 1521-1533.

Fulton D, Gratton JP, McCabe TJ, Fontana J, Fujio Y, Walsh K, *et al.* (1999). Regulation of endothelium-derived nitric oxide production by the protein kinase Akt. *Nature* **399:** 597-601.

Gatti RM, Alvarez B, Vasquez-Vivar J, Radi R, Augusto O (1998). Formation of spin trap adducts during the decomposition of peroxynitrite. *Arch Biochem Biophys* **349:** 36-46.

Giraldez RR, Zweier JL (1998). An improved assay for measurement of nitric oxide synthase activity in biological tissues. *Anal Biochem* **261:** 29-35.

Gopalakrishnan B, Nash KM, Velayutham M, Villamena FA (2012). Detection of nitric oxide and superoxide radical anion by electron paramagnetic resonance spectroscopy from cells using spin traps. *J Vis Exp***:** e2810.

Gross SS, Wolin MS (1995). Nitric oxide: pathophysiological mechanisms. *Annu Rev Physiol* **57:** 737-769.

Harris MB, Ju H, Venema VJ, Liang H, Zou R, Michell BJ, *et al.* (2001). Reciprocal phosphorylation and regulation of endothelial nitric-oxide synthase in response to bradykinin stimulation. *J Biol Chem* **276:** 16587-16591.

Heitzer T, Schlinzig T, Krohn K, Meinertz T, Munzel T (2001). Endothelial dysfunction, oxidative stress, and risk of cardiovascular events in patients with coronary artery disease. *Circulation* **104:** 2673-2678.

Hyland K (1985). Estimation of tetrahydro, dihydro and fully oxidised pterins by high-performance liquid chromatography using sequential electrochemical and fluorometric detection. *J Chromatogr* **343:** 35-41.

Ishii M, Shimizu S, Momose K, Yamamoto T (1999). SIN-1-induced cytotoxicity in cultured endothelial cells involves reactive oxygen species and nitric oxide: protective effect of sepiapterin. *J Cardiovasc Pharmacol* **33:** 295-300.

Kizhakekuttu TJ, Widlansky ME (2010). Natural antioxidants and hypertension: promise and challenges. *Cardiovasc Ther* **28:** e20-32.

Kuzkaya N, Weissmann N, Harrison DG, Dikalov S (2003). Interactions of peroxynitrite, tetrahydrobiopterin, ascorbic acid, and thiols: implications for uncoupling endothelial nitric-oxide synthase. *J Biol Chem* **278:** 22546-54.

Lin MI, Fulton D, Babbitt R, Fleming I, Busse R, Pritchard KA Jr, *et al.* (2003). Phosphorylation of threonine 497 in endothelial nitric-oxide synthase coordinates

the coupling of L-arginine metabolism to efficient nitric oxide production. *J Biol Chem* **278:** 44719-44726.

Locigno EJ, Zweier JL, Villamena FA (2005). Nitric oxide release from the unimolecular decomposition of the superoxide radical anion adduct of cyclic nitrones in aqueous medium. *Org Biomol Chem* **3:** 3220-3227.

Lomonosova EE, Kirsch M, Rauen U, de Groot H (1998). The critical role of Hepes in SIN-1 cytotoxicity, peroxynitrite versus hydrogen peroxide. *Free Radic Biol Med* **24:** 522-528.

Martin-Romero FJ, Gutierrez-Martin Y, Henao F, Gutierrez-Merino C (2004). Fluorescence measurements of steady state peroxynitrite production upon SIN-1 decomposition: NADH versus dihydrodichlorofluorescein and dihydrorhodamine 123. *J Fluoresc* **14:** 17-23.

McCabe TJ, Fulton D, Roman LJ, Sessa WC (2000). Enhanced electron flux and reduced calmodulin dissociation may explain "calcium-independent" eNOS activation by phosphorylation. *J Biol Chem* **275:** 6123-6128.

Michell BJ, Chen ZP, Tiganis T, Stapleton D, Katsis F, Power DA, *et al.* (2001). Coordinated control of endothelial nitric-oxide synthase phosphorylation by protein kinase C and the cAMP-dependent protein kinase. *J Biol Chem* **276:** 17625-17628.

Munzel T, Gori T, Bruno RM, Taddei S (2010). Is oxidative stress a therapeutic target in cardiovascular disease? *Eur Heart J* **31:** 2741-2748.

Nash KM, Rockenbauer A, Villamena FA (2012). Reactive nitrogen species reactivities with nitrones: theoretical and experimental studies. *Chem Res Toxicol* **25:** 1581-1597.

O'Donnell VB, Freeman BA (2001). Interactions between nitric oxide and lipid oxidation pathways: implications for vascular disease. *Circ Res* **88:** 12-21.

Okazaki T, Otani H, Shimazu T, Yoshioka K, Fujita M, Iwasaka T (2011). Ascorbic acid and N-acetyl cysteine prevent uncoupling of nitric oxide synthase and increase tolerance to ischemia/reperfusion injury in diabetic rat heart. *Free Radic Res* **45:** 1173-1183.

Rastaldo R, Cappello S, Di Stilo A, Folino A, Losano G, Pagliaro P (2012). A lipophilic nitric oxide donor and a lipophilic antioxidant compound protect rat heart against ischemia-reperfusion injury if given as hybrid molecule but not as a mixture. *J Cardiovasc Pharmacol* **59:** 241-248.

Rockenbauer A, Korecz L (1996). Automatic computer simulations of ESR spectra. *Appl Magn Reson* **10:** 29−43.

Shay KP, Moreau RF, Smith EJ, Smith AR, Hagen TM (2009). Alpha-lipoic acid as a dietary supplement: molecular mechanisms and therapeutic potential. *Biochim Biophys Acta* **1790:** 1149-1160.

Šnyrychová I (2010). Improvement of the sensitivity of EPR spin trapping in biological systems by cyclodextrins: A model study with thylakoids and photosystem II particles. *Free Radic Biol Med* **48:** 264-274.

Tosaki A, Blasig IE, Pali T, Ebert B (1990). Heart protection and radical trapping by DMPO during reperfusion in isolated working rat hearts. *Free Radic Biol Med* **8:** 363-372.

Traynham CJ, Roof SR, Wang H, Prosak RA, Tang L, Viatchenko-Karpinski S, *et al.* (2012). Diesterified nitrone rescues nitroso-redox levels and increases myocyte contraction via increased SR Ca2+ handling. *PLOS One* **7:** e52005.

Vasquez-Vivar J, Martasek P, Whitsett J, Joseph J, Kalyanaraman B (2002). The ratio between tetrahydrobiopterin and oxidized tetrahydrobiopterin analogues controls superoxide release from endothelial nitric oxide synthase: an EPR spin trapping study. *Biochem J* **362:** 733-739.

Villamena FA, Das A, Nash KM (2012). Potential implication of the chemical properties and bioactivity of nitrone spin traps for therapeutics. *Future Med Chem* **4:** 1171-1207.

Villamena FA, Hadad CM, Zweier JL (2005). Comparative DFT study of the spin trapping of methyl, mercapto, hydroperoxy, superoxide, and nitric oxide radicals by various substituted cyclic nitrones. *J Phys Chem A* **109:** 1662-1674.

Villamena FA, Zweier JL (2004). Detection of reactive oxygen and nitrogen species by EPR spin trapping. *Antioxid Redox Signal* **6:** 619-629.

Vita JA (2011). Endothelial function. *Circulation* **124:** e906-912.

Wang PG, Cai TB, Taniguchi N (2005). Nitric oxide donors. Weinheim: Wiley-VCH Verlag GmbH & Co.

Wei CC, Crane BR, Stuehr DJ (2003). Tetrahydrobiopterin radical enzymology. *Chem Rev* **103:** 2365-2383.

Willcox BJ, Curb JD, Rodriguez BL (2008). Antioxidants in cardiovascular health and disease: key lessons from epidemiologic studies. *Am J Cardiol* **101:** 75D-86D.

Xia Y, Dawson VL, Dawson TM, Snyder SH, Zweier JL (1996). Nitric oxide synthase generates superoxide and nitric oxide in arginine-depleted cells leading to peroxynitrite-mediated cellular injury. *Proc Natl Acad Sci U S A* **93:** 6770-6774.

Xia Y, Tsai AL, Berka V, Zweier JL (1998). Superoxide generation from endothelial nitric-oxide synthase. A Ca2+/calmodulin-dependent and tetrahydrobiopterin regulatory process. *J Biol Chem* **273:** 25804-25808.

Xia Y, Zweier JL (1997). Direct measurement of nitric oxide generation from nitric oxide synthase. *Proc Natl Acad Sci U S A* **94:** 12705-12710.

Zamora PL, Villamena FA (2013). Pharmacological approaches to the treatment of oxidative stress-induced cardiovascular dysfunctions. *Future Med Chem* **5:** 465-478.

Zuo L, Chen YR, Reyes LA, Lee HL, Chen CL, Villamena FA, *et al.* (2009). The radical trap 5,5-dimethyl-1-pyrroline N-oxide exerts dose-dependent protection against myocardial ischemia-reperfusion injury through preservation of mitochondrial electron transport. *J Pharmacol Exp Ther* **329:** 515-523.

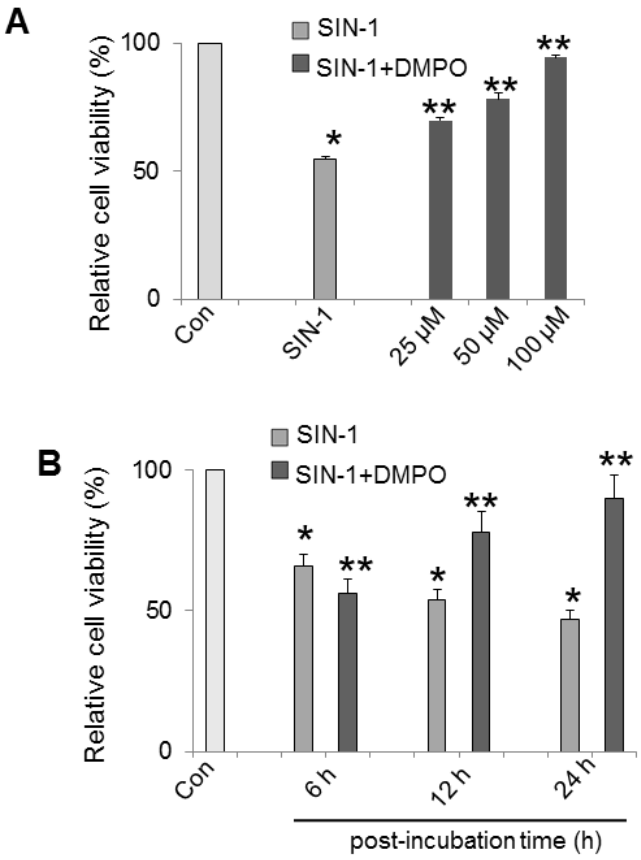
A
SIN-1
SIN-1+DMPO
Relative cell viability (%)
100
50
0
*
**
**
**
Con
SIN-1
25 μM
50 μM
100 μM
B
SIN-1
SIN-1+DMPO
Relative cell viability (%)
100
50
0
*
**
*
**
*
**
Con
6 h
12 h
24 h
post-incubation time (h)

Figure 1

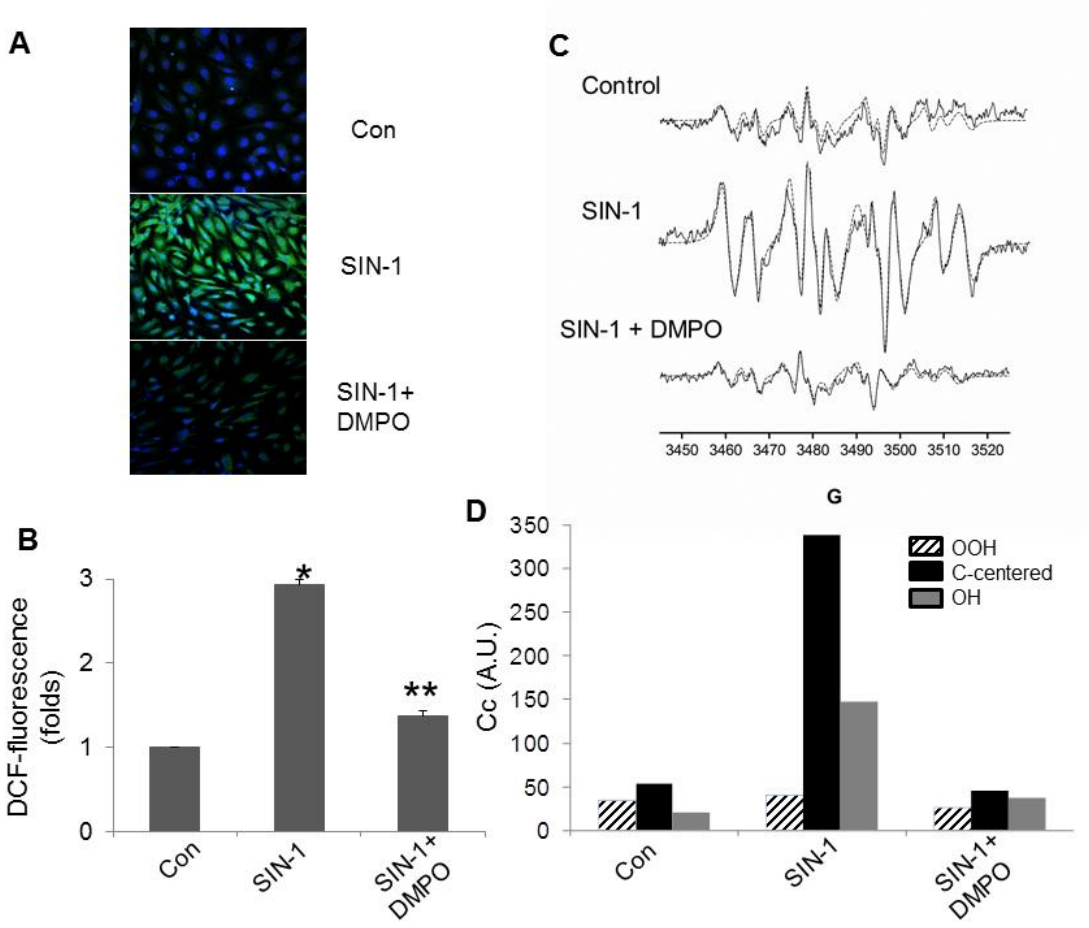
A
Con
SIN-1
SIN-1+
DMPO
C
Control
SIN-1
SIN-1 + DMPO
3450 3460 3470 3480 3490 3500 3510 3520
B
DCF-fluorescence
(folds)
0
1
2
3
*
**
Con
SIN-1
SIN-1+
DMPO
D
G
Cc (A.U.)
0
50
100
150
200
250
300
350
OOH
C-centered
OH
Con
SIN-1
SIN-1+
DMPO

Figure 2

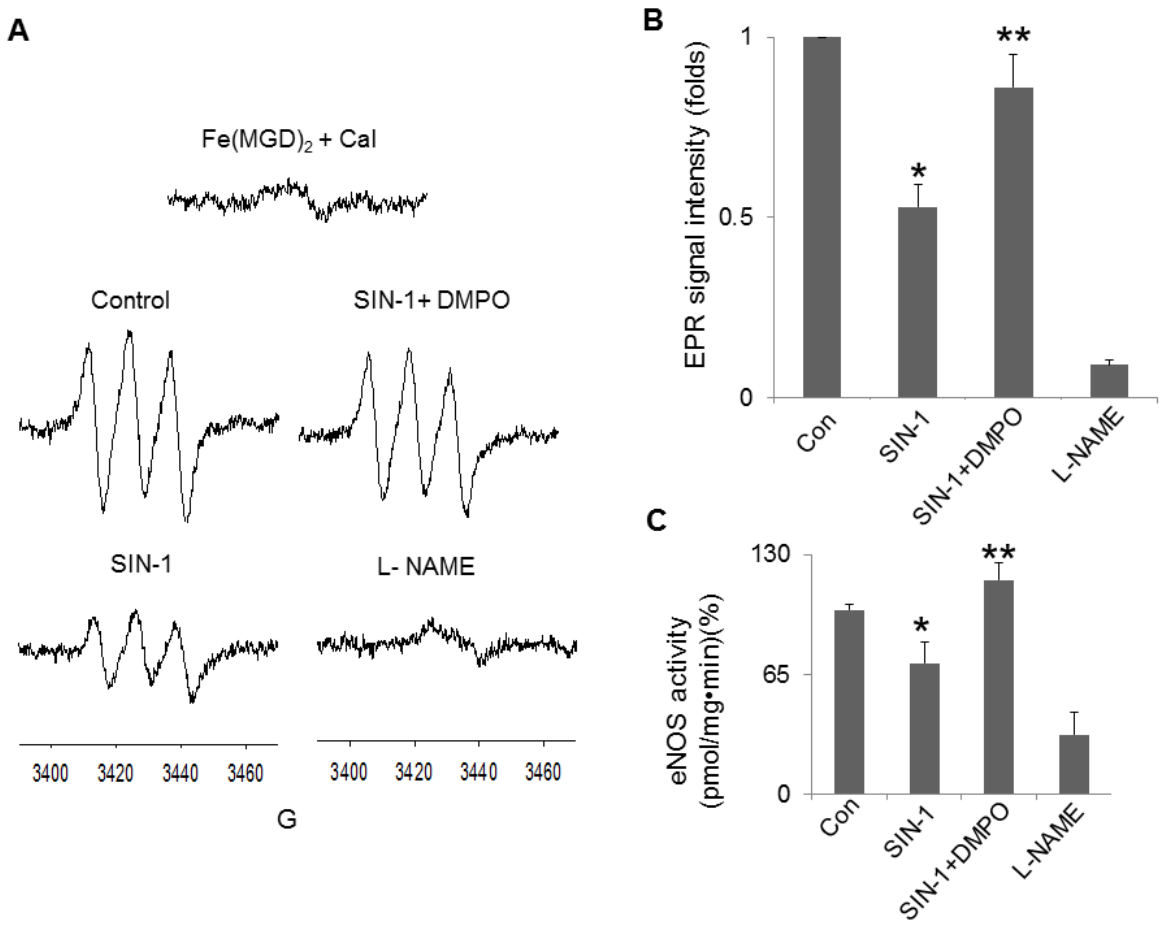
A
Fe(MGD)2 + Cal
Control
SIN-1+ DMPO
SIN-1
L- NAME
3400
3420
3440
3460
G
B
EPR signal intensity (folds)
1
0.5
0
*
**
Con
SIN-1
SIN-1+DMPO
L-NAME
C
eNOS activity
(pmol/mg•min)(%)
130
65
0
*
**
Con
SIN-1
SIN-1+DMPO
L-NAME

Figure 3

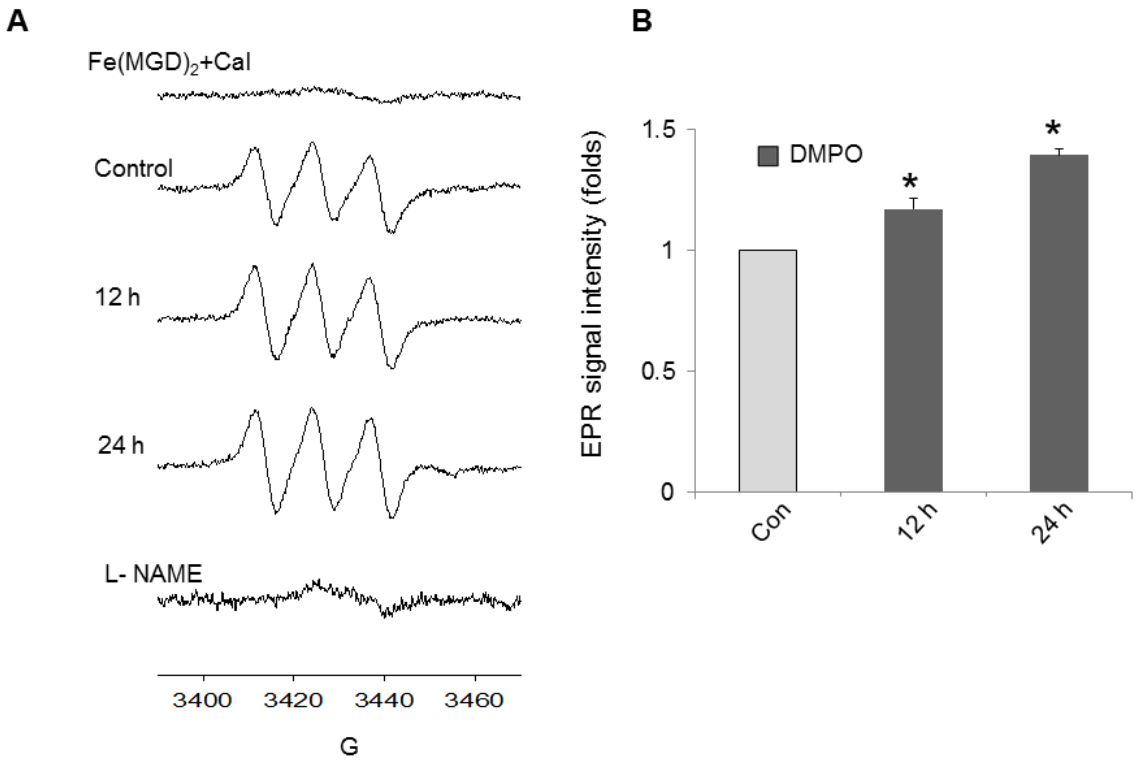
A
Fe(MGD)2+Cal
Control
12 h
24 h
L- NAME
3400
3420
3440
3460
G
B
EPR signal intensity (folds)
1.5
1
0.5
0
DMPO
*
*
Con
12 h
24 h

Figure 4

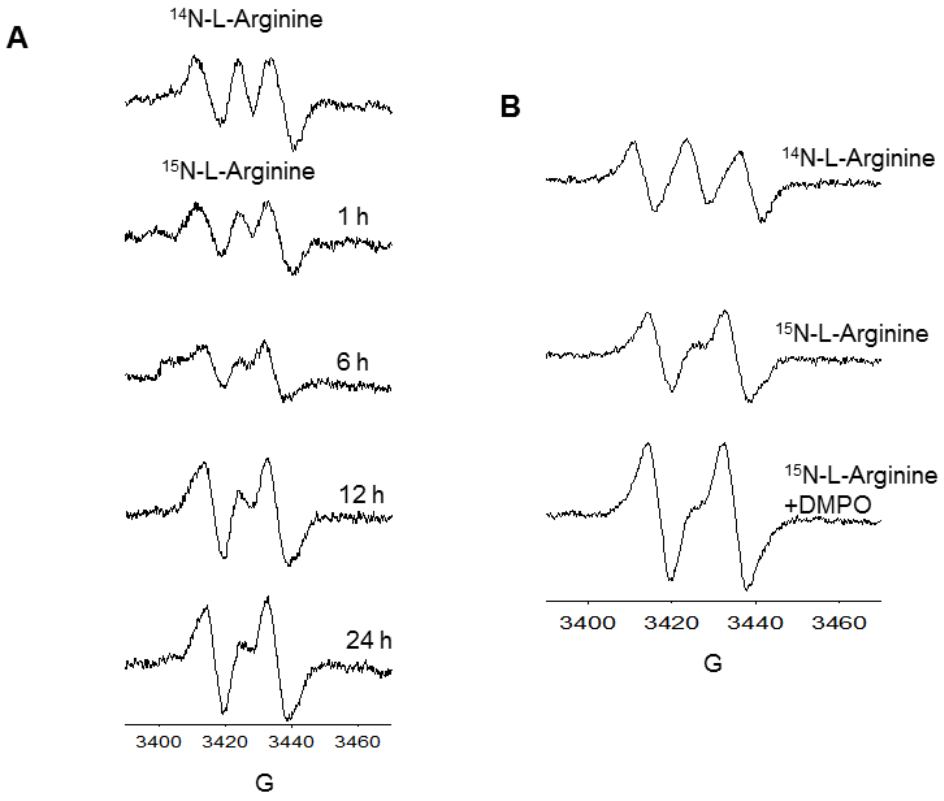
A
^{14}N-L-Arginine
^{15}N-L-Arginine
1 h
6 h
12 h
24 h
3400
3420
3440
3460
G
B
^{14}N-L-Arginine
^{15}N-L-Arginine
^{15}N-L-Arginine
+DMPO
3400
3420
3440
3460
G

Figure 5

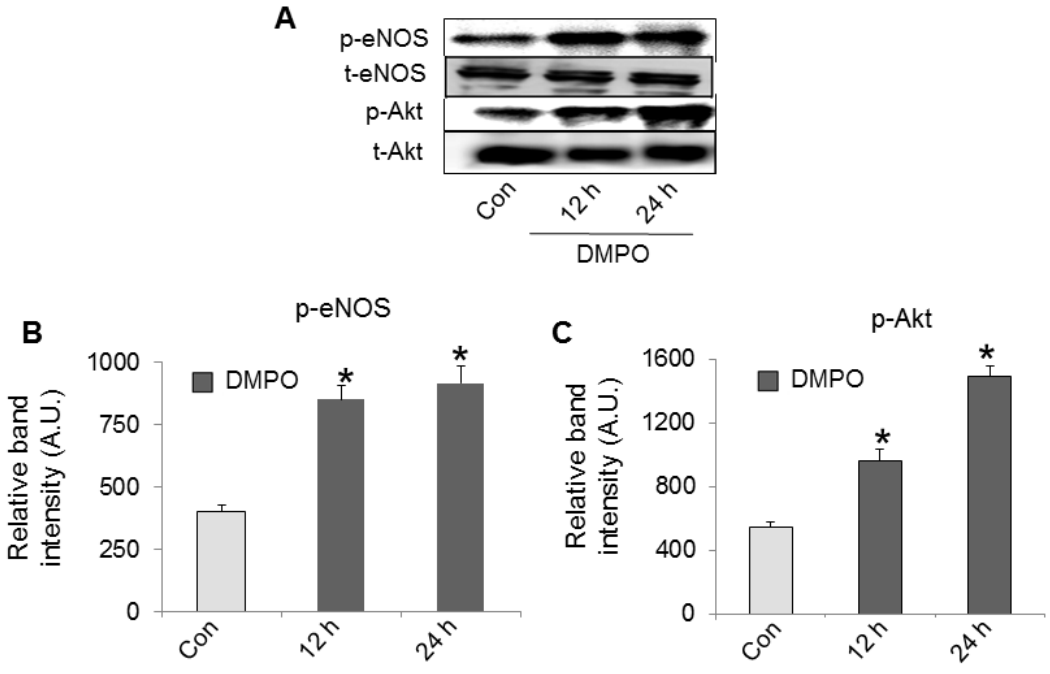
A
p-eNOS
t-eNOS
p-Akt
t-Akt
Con
12 h
24 h
DMPO
B
p-eNOS
Relative band intensity (A.U.)
1000
750
500
250
0
DMPO
*
*
Con
12 h
24 h
C
p-Akt
Relative band intensity (A.U.)
1600
1200
800
400
0
DMPO
*
*
Con
12 h
24 h

Figure 6

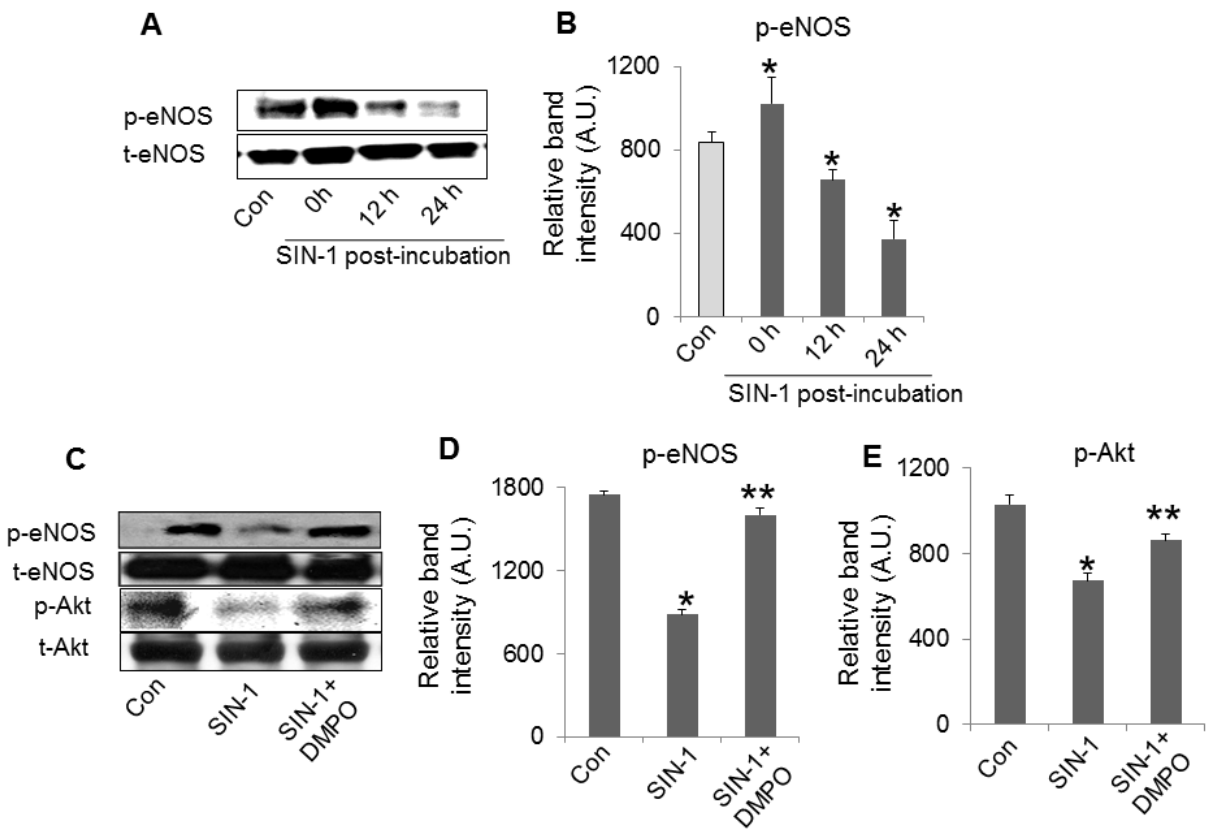
A
p-eNOS
t-eNOS
Con
0h
12 h
24 h
SIN-1 post-incubation
B
p-eNOS
Relative band intensity (A.U.)
1200
800
400
0
Con
0 h
12 h
24 h
SIN-1 post-incubation
C
p-eNOS
t-eNOS
p-Akt
t-Akt
Con
SIN-1
SIN-1+ DMPO
D
p-eNOS
Relative band intensity (A.U.)
1800
1200
600
0
Con
SIN-1
SIN-1+ DMPO
E
p-Akt
Relative band intensity (A.U.)
1200
800
400
0
Con
SIN-1
SIN-1+ DMPO

Figure 7

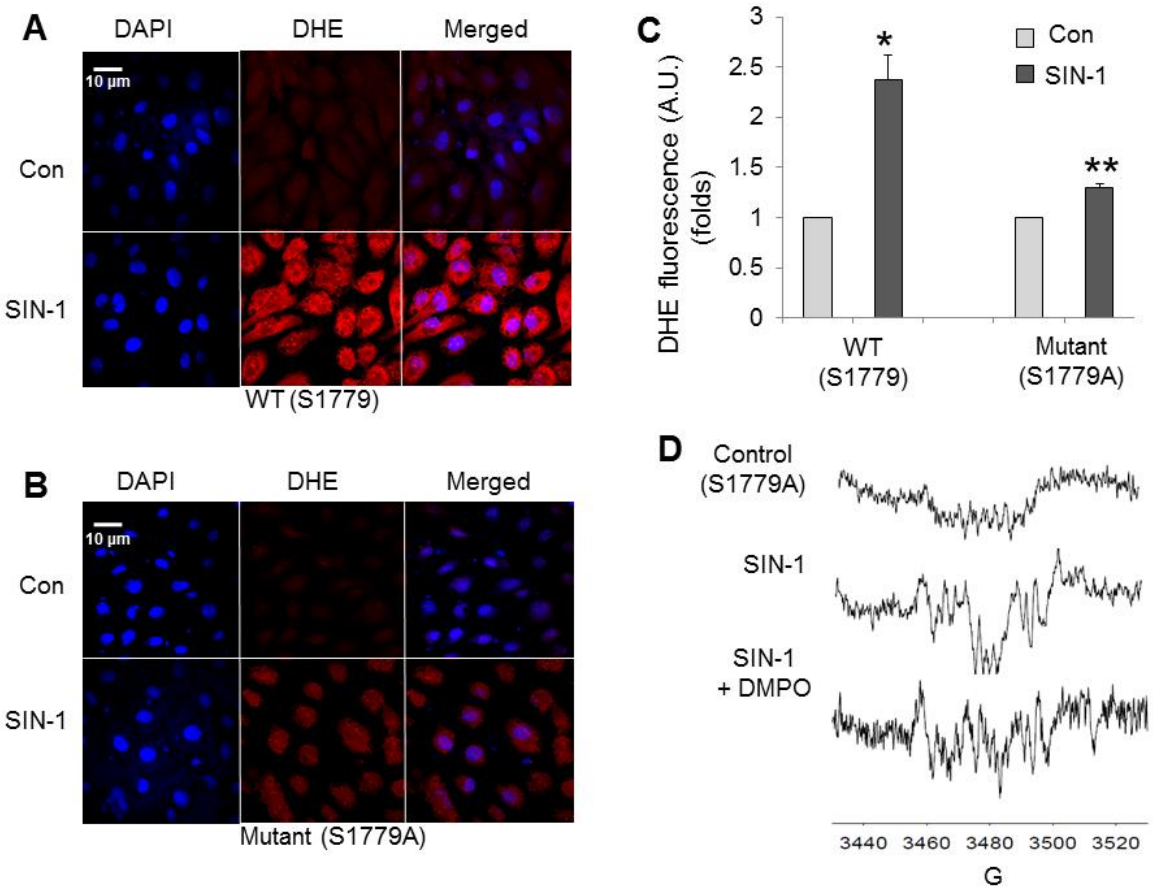
A
DAPI
DHE
Merged
10 μm
Con
SIN-1
WT (S1779)
B
DAPI
DHE
Merged
10 μm
Con
SIN-1
Mutant (S1779A)
C
DHE fluorescence (A.U.) (folds)
3
2.5
2
1.5
1
0.5
0
*
**
Con
SIN-1
WT (S1779)
Mutant (S1779A)
D
Control (S1779A)
SIN-1
SIN-1 + DMPO
3440
3460
3480
3500
3520
G

Figure 8

Figure Captions

Figure 1. Effect of DMPO on SIN-1 induced cytotoxicity. (A) Dose-dependence. (B) Time-dependence. Measured using MTT assay. All data are represented as the mean ± SEM, *p < 0.05 vs. control (untreated cells), **p < 0.05 vs. SIN-1 treated cells, where n = 6.

Figure 2. Effect of DMPO on SIN-1 induced ROS generation in BAEC. (A) Confocal micrographs of ROS generation in BAEC treated with SIN-1 (500 μM) alone and those post-incubated with DMPO (100 μM). (B) Plot of average DCF- fluorescence obtained from 100 cells. All data are represented as mean ± SEM, *p < 0.05 vs. control (untreated cells), **p < 0.05 vs. SIN-1 treated cells, where n = 3. (C) Representative X-band EPR spectra and simulated (dotted lines) of radical adducts formed in SIN-1 treated BAEC, with and without DMPO (100 μM) incubation using EMPO/Me-β–CD as spin trap (see Table S2 for complete simulated EPR parameters). (D) Plot of the concentrations of the $HO_2^{\bullet}$, $HO^{\bullet}$ and C-centered adducts from Figure 2C.

Figure 3. Restoration of NO production and eNOS activity in SIN-1 treated BAEC by DMPO. (A) X-band EPR spectra of NO using $Fe(MGD)_2$ spin trap generated form SIN-1 treated BAEC and with or without post-incubation with DMPO (100 μM). (B) Plot of the relative low field EPR peak intensity of $Fe(MGD)_2$-NO. (C) eNOS activity as measured by arginine to citrulline assay from BAEC treated with SIN-1 with and without

DMPO incubation. All data are represented as mean ± SEM, *p < 0.05 vs. control (untreated cells), **p < 0.05 vs. SIN-1 treated cells, where n = 3.

Figure 4. Time-dependent increase in NO production in DMPO-treated BAEC. (A) X-band EPR spectra of NO using $Fe(MGD)_2$ spin trap generated in BAEC during 0 to 24 h of incubation with DMPO (100 μM) and NOS inhibitor, L-NAME. (B) Plot of the relative low field EPR peak intensity of $Fe(MGD)_2$-NO. Results are represented as mean ± SEM, *p < 0.05 vs. control (untreated cells), where n = 3.

Figure 5. Determination of the source of NO. (A) X-band EPR spectra of ^{15}NO–Fe–MGD showing the characteristic doublet peak produced from BAEC supplemented with L-[^{15}N] arginine at various incubation times. (B) EPR spectra of NO adducts formed from BAEC incubated alone in medium containing L-[^{14}N] arginine; L-[^{15}N] arginine containing medium; and L-[^{15}N] arginine containing medium supplemented with DMPO. All experiments were performed at least n = 3.

Figure 6. Effect of DMPO on the phosphorylation status of eNOS and AKT proteins in BAEC. (A) Western blot expression levels of p-eNOS, total eNOS, p-Akt, and t-Akt in BAEC treated with 100 μM DMPO at 12 h and 24 h incubation. Densitometric analysis of the expression levels of (B) p-eNOS (B) and (C) p-Akt. All data are represented as mean ± SEM, *p < 0.05 vs. control (untreated cells), where n = 3.

Figure 7. Modulation of eNOS and Akt phosphorylation by DMPO in SIN-1 treated cells. (A) Western blot analysis; and (B) densitometric analysis of p-eNOS S1179 and t-

eNOS expression levels in BAEC treated with SIN-1 (500 μM, 2 h) and post incubated in plain media (without SIN-1) at various incubation times. Results are represented as mean ± SEM,*p < 0.05 vs. control (untreated cells). (C) Western blot analysis of p-eNOS S1179, t-eNOS, p-Akt (ser 473) and t-Akt expression in BAEC treated with SIN-1 (500 μM) alone and post-incubated with DMPO (100 μM). Densitometric analysis of the expression levels of (D) p-eNOS S1179 and (E) p-Akt from the above mentioned conditions. Results are represented as mean ± SEM, *p < 0.05 vs. control (untreated cells), **p < 0.05 vs. SIN-1 treated cells, where n = 3.

Figure 8. Detection of ROS generation in wild type and mutant eNOS cDNA-transfected HEK293 cells in the presence of SIN-1. Confocal DHE and DAPI images of untreated and SIN-1 treated HEK293 cells transfected with cDNAs encoding (A) wild type eNOS S1179; (B) mutant eNOS cDNA S1179A. (C) Plot of relative average DHE-fluorescence intensities (n = 100 cells). Data are represented as mean ± SEM, *p < 0.05 vs. control (non-transfected cells) and **p < 0.05 vs. SIN-1 treated wild type eNOS S1179 transfected cells. (D) X-band EPR detection of radical generation using EMPO/Me-β–CD from mutant eNOS cDNA transfected HEK293 cells that are untreated (top) and treated with SIN-1 (middle), and post-incubated with DMPO (bottom). All experiments were performed in triplicates.